

Article

Removal of Organic Micropollutants from a Municipal Wastewater Secondary Effluent by UVA-LED Photocatalytic Ozonation

Ana M. Chávez ¹, Ana R. Ribeiro ², Nuno F. F. Moreira ², Adrián M. T. Silva ^{2,*}, Ana Rey ¹, Pedro M. Álvarez ¹ and Fernando J. Beltrán ^{1,*}

¹ Departamento de Ingeniería Química y Química Física, Instituto Universitario de Investigación del Agua, Cambio Climático y Sostenibilidad, Universidad de Extremadura, Avenida de Elvas S/N, 06006 Badajoz, Spain; amchavez@unex.es (A.M.C.); anarey@unex.es (A.R.); pmalvare@unex.es (P.M.Á.)

² Laboratory of Separation and Reaction Engineering - Laboratory of Catalysis and Materials (LSRE-LCM), Faculdade de Engenharia, Universidade do Porto, Rua Dr. Roberto Frias s/n, 4200-465 Porto, Portugal; ritalado@fe.up.pt (A.R.R.); nmoreira@fe.up.pt (N.F.F.M.)

* Correspondence: adrian@fe.up.pt (A.M.T.S.); fbeltran@unex.es (F.J.B.); Tel.: +351-22-041-4531 (A.M.T.S.); +34-924-289387 (F.J.B.)

Received: 29 April 2019; Accepted: 18 May 2019; Published: 22 May 2019



Abstract: Numerous contaminants of emerging concern (CECs) have been found in different water bodies. Directive 2013/39/EU and Decision 2018/840/EU are consequently being implemented in the field of water policies. Twelve CECs (e.g., isoproturon, ciprofloxacin, and clarithromycin are among those listed) were detected in a municipal wastewater secondary effluent by means of solid phase extraction and ultra-high-performance liquid chromatography with tandem mass spectrometry (SPE-UHPLC-MS/MS). Different advanced oxidation processes (AOPs), based on the combination of ozone, UVA-LED and powdered TiO₂, were investigated for their removal in a semi-batch operation. In addition, TiO₂-coated glass rings (P25R) were characterized with different techniques (SEM, WDXRF) and used for continuous mode operation in a packed bed reactor (PBR). Among the AOPs studied, ozone-based processes were found to be more efficient than heterogeneous photocatalysis. A kinetic study was performed showing that direct ozonation is the main oxidation pathway for CEC removal. Ozone was successfully decomposed in combination with UVA-LED and P25R, resulting in an apparent rate constant of $3.2 \times 10^{-2} \text{ s}^{-1}$ higher than in the O₃/LED system ($1.0 \times 10^{-3} \text{ s}^{-1}$) or with ozone alone ($8.6 \times 10^{-5} \text{ s}^{-1}$). Hydroxyl radical reaction could prevail over direct ozone reaction for the most refractory compounds (e.g., isoproturon).

Keywords: municipal wastewater secondary effluent; contaminants of emerging concern; ozonation; light emitting diodes; TiO₂-coated glass rings

1. Introduction

Contaminants of emerging concern (CECs) are continuously discharged into aquatic systems with little or no awareness of their consequences. Pharmaceuticals, pesticides, industrial compounds, natural hormones, and personal care products belong to this group of substances. Although their concentration levels are very low, usually in the ng·L⁻¹ or µg·L⁻¹ range [1–3], biological acute and chronic toxicity in aquatic organisms has been observed [4,5].

To date, the European Union (EU) has established a list of priority substances (Directive 2013/39/EU) and a watch list of CECs that have to be monitored to guarantee water quality (Decision 2015/495/EU, Decision 2018/840/EU) [6–8]. Other CECs are most likely to be included in the watch list in the near future.

Since CECs are difficult to remove by conventional treatments of municipal wastewater treatment plants (MWWTPs), alternative treatment methods such as adsorption, membrane separation, photocatalysis, or ozonation are being investigated [9,10]. Among the oxidation processes applied in this work, ozonation has been shown to be a very effective treatment due to ozone direct reactions with some organics and ozone decomposition (mainly at basic pH) into hydroxyl radical (HO^\bullet), a strong non-selective oxidant radical oxygen species (ROS) [11]. However, decomposition of ozone in water also involves a series of reactions which prevent other less reactive ROS from being able to degrade most of the CECs. To enhance the efficiency of ozonation processes for the degradation of CECs, ozone may be used in combination with certain catalysts and/or radiation sources to promote ozone decomposition into HO^\bullet [12,13]. Reaction mechanisms of these oxidation processes are well known in literature [13] (see main reaction steps of these mechanisms in section S1 of the supplementary information).

In this sense, light emitting diodes (LEDs) represent an attractive and cost-effective alternative because of their long lifetime and high-energy efficiency. Regarding photocatalysts, TiO_2 in powder form has so far been the most commonly used material in photocatalytic oxidation of CECs. However, given the difficult separation of nanosized powered TiO_2 , a great deal of research is recently devoted to the use of immobilized TiO_2 [14].

This work focuses on the removal of some CECs detected in municipal secondary wastewater collected in an MWWTP in Northern Portugal. Combinations of ozone, UVA-LEDs, and P25 TiO_2 (Evonik P25), both in powdered form (P25) and immobilized on glass rings (P25R), were tested as treatment approaches. Two modes of ozonation operation were also investigated: semi-batch (P25 as catalyst) and continuous flow (P25R as catalyst). Some CECs examined in this study (e.g., isoproturon, ciprofloxacin, and clarithromycin) are among those included in Directive 2013/39/EU and Decision 840/2018/EU. The main objectives of this work were: (i) to assess efficiencies of semi-batch and continuous processes and (ii) to determine the importance of direct ozonation and HO^\bullet mediated-reactions in the degradation of the CECs.

2. Results

2.1. CECs Detected in Secondary Effluent Samples

Two wastewater (WW) samples (namely WW1 and WW2) were collected at the outlet of the secondary settling tank of an MWWTP in Northern Portugal (see Table S1 for main WW characteristics). WW1 was used in semi-batch experiments and WW2 in continuous flow runs. Forty-five CEC candidates were analyzed by the solid phase extraction and ultra-high-performance liquid chromatography with tandem mass spectrometry (SPE-UHPLC-MS/MS) validated method (Table S2) and twelve compounds were found in both WW1 and WW2 samples (Table 1): the herbicide isoproturon, and eleven pharmaceutical compounds (bezafibrate, carbamazepine, ciprofloxacin, clarithromycin, clopidogrel, diclofenac, fluoxetine, metoprolol, propranolol, tramadol, and venlafaxine).

While clopidogrel was detected at concentrations below the quantification limit, carbamazepine, ciprofloxacin, diclofenac, isoproturon, tramadol, and venlafaxine were found at $\mu\text{g}\cdot\text{L}^{-1}$ concentration level, thus confirming that the conventional treatment applied at the MWWTP is not efficient enough to eliminate these micropollutants. Of special concern are isoproturon (included in Directive 2013/39/EU), ciprofloxacin (recently added to the latest 2018/840/EU Decision), clarithromycin (included in the first Decision 2015/495/EU and maintained in Decision 2018/840/EU) (Table S2).

Table 1. List of numbered target pollutants found in wastewater (WW) samples and their concentrations.

No.	COMPOUND	Concentration (ng·L ⁻¹)	
		WW1	WW2
1	Bezafibrate	61 ± 1	7.1 ± 0.4
2	Carbamazepine	1284 ± 225	1222 ± 278
3	Ciprofloxacin	4287 ± 1208	138 ± 74
4	Clarithromycin	758 ± 31	94 ± 4
5	Clopidogrel	<MQL	<MQL
6	Diclofenac	1528 ± 17	1268 ± 67
7	Fluoxetine	62 ± 193	257 ± 51
8	Isoproturon	61 ± 7	1827 ± 219
9	Metoprolol	209 ± 13	187 ± 22
10	Propranolol	173 ± 40	61 ± 14
11	Tramadol	1233 ± 40	3439 ± 727
12	Venlafaxine	628 ± 555	1647 ± 359

<MQL.: below method quantification limit.

2.2. Removal of CECs in Semi-Batch Experiments

Figure 1 shows removal of CECs in ozonation (O₃), photolytic ozonation (O₃/LED), photocatalytic oxidation (O₂/LED/P25), and photocatalytic ozonation (O₃/LED/P25) in semi-batch experiments. As can be observed, O₂/LED/P25 (i.e., heterogeneous photocatalysis) barely reached 15% removal of any CEC. In contrast, elimination percentages achieved by ozonation processes were above 90% in all cases except for ciprofloxacin, metoprolol, and propranolol. For ciprofloxacin, percentage removals were 56%, 62%, and 100% by single ozonation, photolytic ozonation, and photocatalytic ozonation, respectively. For the beta-blockers propranolol and metoprolol, which were detected at much lower concentrations, random trends were observed for the different processes and removal efficiencies were much lower (for instance, 43% and 16% were respectively achieved with photocatalytic ozonation).

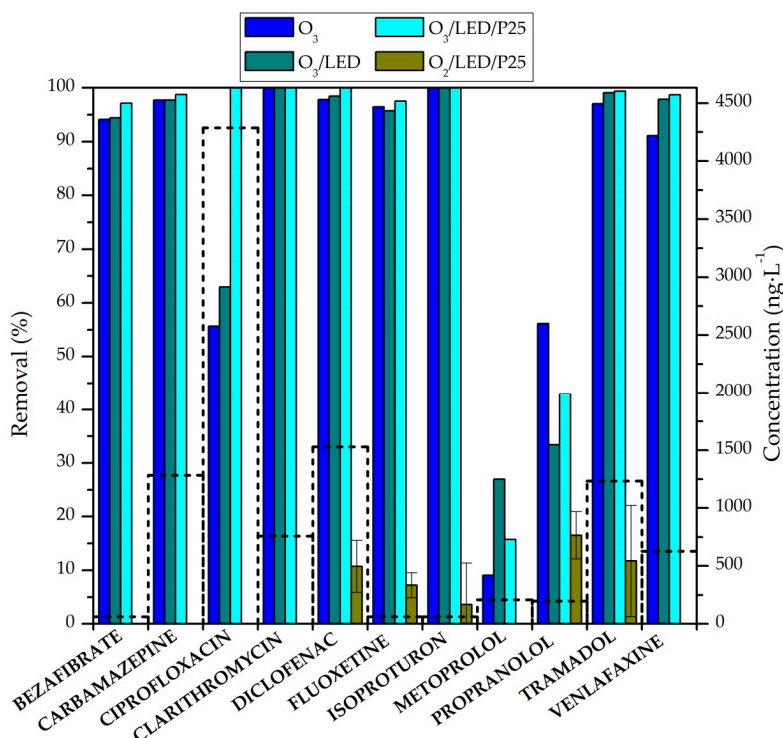


Figure 1. Removal of contaminants of emerging concern (CECs)s from wastewater 1 (WW1) (left axis, solid bars) and initial concentration of CECs (right axis, dotted bars) in different semi-batch experiments (ozonation (O₃), photolytic ozonation (O₃/LED), photocatalytic oxidation (O₂/LED/P25), and photocatalytic ozonation (O₃/LED/P25)). Conditions: reaction time = 10 min; gas flow rate = 150 mL·min⁻¹; P25 loading (when applied) = 0.5 g·L⁻¹ ozone concentration (when applied) = 50 mg·L⁻¹.

With regard to the substances on the priority and watch lists, isoproturon and clarithromycin were completely removed by the three ozone-based processes, whereas ciprofloxacin was totally removed by photocatalytic ozonation. The effect is strongly marked due to its higher concentration in WW1. Similar trends are seen in particular for those CECs whose concentrations were above $1000 \text{ ng}\cdot\text{L}^{-1}$ (Table 1).

To ascertain the effect of suspended matter on removal efficiency of CECs, a series of runs with filtered WW1 samples were carried out. As has been reported [15], filtration did not enhance the performance of these processes in terms of removal of CECs (see Figure S1).

2.3. Continuous Flow Experiments

A preliminary residence time distribution (RTD) analysis was carried out to model flow pattern in the packed photo-reactor used for continuous flow experiments. Two possible scenarios were hypothesized regarding the flow model to be used (Figure S3): a) a perfectly mixed reactor and b) two perfectly mixed reactors in series corresponding to the column reactor and the recirculation column. Figure S4 shows the experimental F curve obtained together with the calculated F curves inferred from the two assumed models. The experimental F curve perfectly agrees with the calculated one corresponding to a perfectly mixed reactor. Taking this information into account, the mean residence time was expected to be 39 min (see Section S2 of Supporting Materials for details).

2.3.1. Characterization of the Immobilized Photocatalyst

SEM images of P25R (Figure S5) were taken from glass rings vertically placed in the microscope chamber, showing the roughness of P25 layers in coated glass rings. Nearly 5 μm of layer thickness was determined in both the polished ring border and the scratched ring surface. WDXRF results (Table S3) show that ca. 0.16 wt. % of TiO_2 was immobilized on the glass rings. This composition was similar in fresh P25R, and after the photocatalytic oxidation and photocatalytic ozonation processes.

2.3.2. Removal of CECs

Photolysis (O_2/LED), photocatalytic oxidation ($\text{O}_2/\text{LED}/\text{P25R}$), ozonation (O_3), photolytic ozonation (O_3/LED), and photocatalytic ozonation ($\text{O}_3/\text{LED}/\text{P25R}$) experiments were carried out with WW2. Figure 2 presents the results obtained in terms of removal of CECs (%), with the exception of bezafibrate, which was not considered in this part of the study due to its very low concentration in this sample (WW2), which was close to the method quantification limit. Photolysis led to different degrees of removal depending on the specific CEC: from no removal at all (in the case of clarithromycin and ciprofloxacin) to a maximum removal of 37% for fluoxetine. Photocatalytic oxidation improved these figures to some extent. With this system, ciprofloxacin reached nearly 100% elimination, though removals of the other CECs were moderate, between 58% for carbamazepine, and approximately 28% for propranolol and clarithromycin. In agreement with the results obtained in semi-batch experiments, the highest removals were obtained with the ozone-based processes (O_3 , O_3/LED , and $\text{O}_3/\text{LED}/\text{P25R}$), for which removal percentages of more than 90% were observed in all the cases. Photocatalytic ozonation was particularly effective with removal of any CEC with percentages higher than 99.9%, except for carbamazepine with 99.2% elimination.

$\text{SUVA}_{254\text{nm}}$ (specific ultraviolet absorbance at 254 nm) is an important variable to be measured in wastewater since it can be considered a surrogate parameter of the presence of aromatic and unsaturated compounds [16]. Figure 3 shows the values of $\text{SUVA}_{254\text{nm}}$ measured at steady state of continuous runs. A decrease in $\text{SUVA}_{254\text{nm}}$ was found as a result of the application of ozone-based processes, especially those involving light, whereas photocatalytic oxidation had no effect on this parameter. Conversely, WW treated with UVA (no catalyst or ozone added) led to an increase in $\text{SUVA}_{254\text{nm}}$. In this case, some intermediates can be formed, which would absorb more radiation as a consequence of their direct photolysis. When both light and catalyst are simultaneously applied, this effect disappears probably due to the formation of $\text{HO}\cdot$. In ozone-based processes, the fast reaction of

ozone and HO^\bullet with unsaturated moieties present in the wastewater could explain the $\text{SUVA}_{254\text{nm}}$ decrease. Decrease of $\text{SUVA}_{254\text{nm}}$ with time clearly shows the decrease of intermediate concentrations and the beneficial effects of ozone processes application compared to photocatalytic oxidation. On the other hand, both pH and dissolved organic carbon (DOC) remain practically unaltered (not shown).

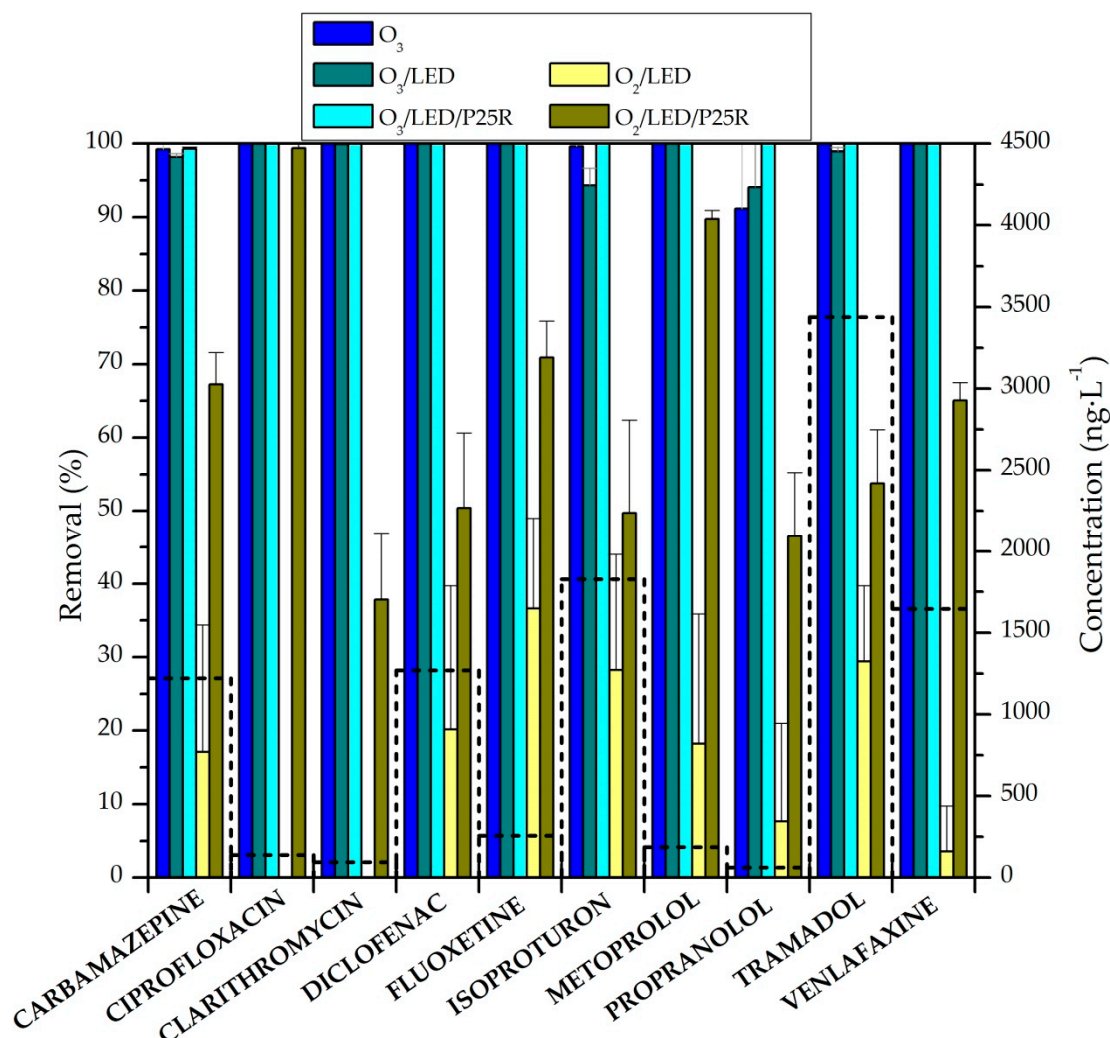


Figure 2. Average removal at steady-state (left axis, solid bars) and inlet concentrations of CECs (right axis, dotted bars) in different continuous flow experiments. Conditions: Hydraulic retention time (HRT) = 39 min; recirculation ratio = 9:10; gas flow rate = $150 \text{ mL}\cdot\text{min}^{-1}$; ozone gas concentration (when applied) = $20 \text{ mg}\cdot\text{L}^{-1}$; P25R loading c.a. 0.29 g .

Results previously reported of CECs removal in secondary urban wastewater doped at some mgL^{-1} , [17–20] also show similar CECs elimination rates when different ozone processes are applied. This confirms that, as far as CECs removal is concerned, direct ozone reactions are likely the main responsible mechanism of oxidation (see later Section 2.4). For instance, Encinas et al. [17] studied a mixture of nine CECs (metoprolol and diclofenac among them) in a secondary urban wastewater with $\text{O}_2/\text{UVA}/\text{TiO}_2$, O_3 , and $\text{O}_3/\text{UVA}/\text{TiO}_2$ systems. CECs, doped at concentrations of 10 mgL^{-1} were removed with similar rates in less than 30 min in ozone processes while photocatalytic oxidation took 120 min to reduce CECs concentration in 20–30%. In another work, this time with solar radiation, Marquez et al. [18] studied the removal of four CECs (atenolol, hydrochlorotiazide, ofloxacin, and trimethoprim) in a secondary urban wastewater. The advanced oxidation process (AOP) applied were $\text{O}_2/\text{Sun}/\text{TiO}_2$, O_3 , O_3/TiO_2 , O_3/Sun , and $\text{O}_3/\text{Sun}/\text{TiO}_2$. With CEC concentrations of 10 mgL^{-1} and ozone dose of 20 mgL^{-1} ozone processes needed less than 25 min for total removal of CECs while

$O_2/Sun/TiO_2$ required more than 3 h with the exception of ofloxacin that needed 2 h. It should be noted that in these works [17–20], due to analytical equipment limitations, total removal of CECs was reducing their concentration below the quantification limit that was some μgL^{-1} .

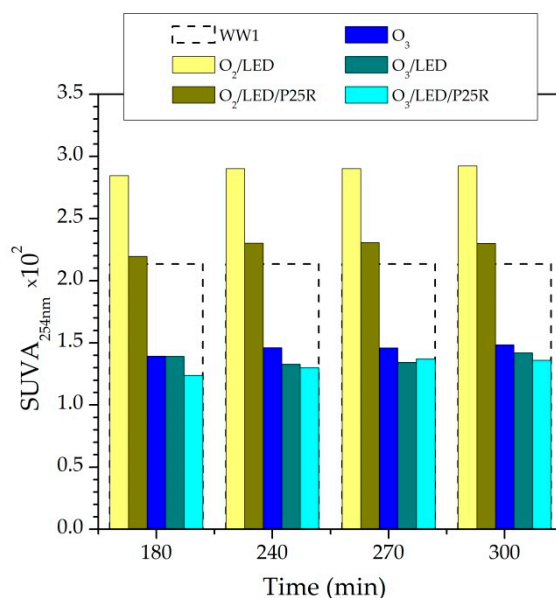


Figure 3. SUVA (specific ultraviolet absorbance) values at 254 nm reached with each oxidation process after different times once the steady state situation was achieved. Conditions: Hydraulic retention time (HRT) = 39 min; recirculation ratio = 9:10; gas flow rate = $150 mL \cdot min^{-1}$; ozone gas concentration (when applied) = $20 mg \cdot L^{-1}$; P25R loading c.a. $0.29 g$.

According to results of Figures 1 and 2 the presence of TiO_2 and LED in an ozone process only adds a small advantage to remove some CECs. However, contributions of simultaneous ozone, radiation, and TiO_2 application is deduced from the higher elimination of total organic carbon (TOC) as reported in previous works [17–20]. In these works, TOC could be followed because of the higher concentrations of initial CECs (doped at mgL^{-1}). To give an example, in the work of Marquez et al. [18], above mentioned, application of O_3 and $O_3/Sun/TiO_2$ systems lead to 38% and 80% TOC removed, respectively, after 3 h treatment in ultrapure water. In our work, TOC measurements were mainly due the water matrix components because of TOC contribution of CECs present was negligible. Then, no conclusion can be made about TiO_2 and LED addition to improve TOC removal of CECs. Another advantage of photocatalytic ozonation, related to the economy of the process, is the lower consumption of ozone to remove a given amount of organic carbon compared to ozonation. For instance, Espejo et al. [19] reported a consumption of 36 and 17 $mg O_3/mg TOC$ with O_3 and $O_3/UVA/Fe_2O_3$ systems, respectively, after 30 min reaction, corresponding to the treatment of nine CECs in a secondary urban wastewater.

2.4. Kinetic Modelling Aspects

This section focuses only on ozone processes since these were the most efficient in removing the CECs. According to the literature, contaminants are mainly removed on reacting with ozone and HO^\bullet [11]. Given that the reacting system behaves as a continuous stirred tank reactor (CSTR), the mass balance of each CEC is given by Equation (1):

$$C_{CEC_0} - C_{CEC} = (k_D C_{O_3} C_{CEC} + k_{HO} C_{HO} C_{CEC}) t_m, \quad (1)$$

where t_m is hydraulic residence time (HRT), k_D and k_{HO} are the rate constants of the reactions of ozone and HO^\bullet with each CEC (see Table 2), C_{CEC_0} is the inlet CEC concentration and C_{CEC} , C_{O_3} , and C_{HO} are the outlet concentrations of CEC, ozone, and HO^\bullet , respectively.

Since most of the HO• comes from the decomposition of ozone [11,13,21], the concentration of any CEC can be expressed as a function of ozone concentration by introducing the R_{ct} factor (ratio of the exposures of HO• and O₃) [22]. Thus, Equation (1) becomes:

$$C_{CEC_0} - C_{CEC} = (k_D + k_{HO}R_{ct})C_{CEC}C_{O_3}t_m = k_T C_{CEC}C_{O_3}t_m, \quad (2)$$

or in terms of conversion of CEC (X):

$$X = k_T(1 - X)C_{O_3}t_m. \quad (3)$$

Table 2. List of numbered CECs, rate constants of their reactions with ozone and hydroxyl radical (HO•) and Ha numbers.

No.	COMPOUND	Rate Constants (M ⁻¹ s ⁻¹)				Ha _D × 10 ⁴	
		k _D	Ref.	k _{HO} × 10 ⁻⁹	Ref.	WW1	WW2
1	Bezafibrate	4.2 × 10 ³	[21]	7.9	[23]	0.3	0.11
2	Carbamazepine	3.0 × 10 ⁵	[23]	8.8	[23]	15.6	15.2
3	Ciprofloxacin	1.9 × 10 ⁴	[24]	4.1	[24]	6.1	1.1
4	Clarithromycin	4.0 × 10 ⁴	[25]	5.0	[25]	2.5	0.9
5	Clopidogrel	unknown		unknown		n.d.*	n.d.*
6	Diclofenac	3.0 × 10 ⁶	[23]	7.5	[23]	48.2	43.9
7	Fluoxetine	3.2 × 10 ⁴	[26]	9.6	[27]	1.0	2.0
8	Isoproturon	2.2 × 10 ³	[28]	7.9	[28]	0.3	1.7
9	Metoprolol	1.4 × 10 ³	[29]	6.8	[29]	0.4	0.4
10	Propranolol	1.0 × 10 ⁵	[30]	10.0	[30]	3.4	1.9
11	Tramadol	4.0 × 10 ³	[25]	6.3	[25]	1.7	2.8
12	Venlafaxine	8.5 × 10 ³	[25]	10.0	[25]	1.7	2.8

n.d.*: not determined; For Hatta number (see Equation (6)): k_L: 1 × 10⁻³ m s⁻¹ [31]; D_{O3}: 1.5 × 10⁻⁹ m² s⁻¹ [32].

Application of Equation (3) to the experimental results should permit determination of k_T for each contaminant. However, this was only possible for some cases of single ozonation or photolytic ozonation, where full conversion of some CECs was not achieved (Figure 2), namely propranolol (ozonation, 90%, or photolytic ozonation, 93% conversions) and isoproturon (photolytic ozonation, 94% conversion). For these CECs, values of k_T were 486, 1653, and 1736 M⁻¹·s⁻¹, respectively. These values are lower than those reported in the literature for the rate constants of the ozone direct reactions (k_D) (Table 2). These apparently contradictory results suggest that direct ozonation is the main mechanism for the removal of these contaminants. This agrees with the fact that ozone-based processes lead to similar conversions, regardless of the use of radiation and/or catalyst (see Figure 2). In addition, this conclusion was confirmed, as shown later, through determination of the ozone kinetic regimes and comparison of the oxidation rates of a given CEC with ozone and HO•.

Because of the high conversions of CECs reached in the continuous ozone-based processes, the mass balance of CEC was also applied to semi-batch experiments. The CEC mass balance in this case leads to Equation (4):

$$- \frac{dC_{CEC}}{dt} = k_T C_{CEC} C_{O_3}. \quad (4)$$

Integration of Equation (4) after variable separation gives:

$$\ln \frac{C_{CEC}}{C_{CEC_0}} = k_T \int_0^t C_{O_3} dt. \quad (5)$$

According to Equation (5), k_T can be obtained from the ratio between the left-hand side of Equation (5) and the ozone exposure (∫C_{O3} dt). Nevertheless, Equation (5) could only be applied to ciprofloxacin, metoprolol, propranolol, and venlafaxine, owing to the fact that conversions lower than 95% were

achieved (Figure 1). As observed, values of k_T obtained (Table 3) are also lower than those of k_D reported for the different ozone-contaminant reactions, which leads us to the conclusion that direct reactions are mainly responsible for contaminant removals in the WW samples studied.

Table 3. Apparent rate constant values of the ozonation process in semi-continuous operation.

Compounds	k_{T-O_3} ($M^{-1}\cdot s^{-1}$)	$k_{T-O_3/LED}$ ($M^{-1}\cdot s^{-1}$)	$k_{T-O_3/LED/P25}$ ($M^{-1}\cdot s^{-1}$)
Ciprofloxacin	730	376	-
Metoprolol	85	119	69
Propranolol	739	154	226
Venlafaxine	2173	1465	1750

Direct Ozonation as the Main Oxidation Pathway of CEC

Following recently reported reasoning [33], kinetic regimes of ozone reactions with the contaminants studied and ozone initiation reaction for the formation of HO^\bullet were evaluated. This required the determination of the Hatta number (Ha) of these reactions (Table 2). For second order irreversible reactions, such as those between ozone and the CECs, Ha_D is defined as:

$$Ha_D = \frac{\sqrt{k_D C_M D_{O_3}}}{k_L}, \quad (6)$$

where D_{O_3} is ozone diffusivity in the liquid phase and k_L is the individual liquid phase mass-transfer coefficient at the reacting conditions. According to Johnson and Davis (1996), ozone diffusivity in water is $1.5 \times 10^{-9} \text{ m}^2\cdot\text{s}^{-1}$ while a value of $10^{-3} \text{ m}\cdot\text{s}^{-1}$ was given for k_L [31,32].

On the other hand, Ha for the initial ozone decomposition reaction into HO^\bullet , a pseudo first order irreversible reaction, is calculated as follows:

$$Ha_I = \frac{\sqrt{k_d D_{O_3}}}{k_L}. \quad (7)$$

In this case, k_d is the corresponding rate constant which varies according to the nature of the ozone process. Thus, for single ozonation, $k_d = 70 \times 10^{\text{pH}-14} \text{ s}^{-1}$, while for photolytic and photocatalytic ozonation apparent k_d values were experimentally determined in this work. For that purpose, a series of continuous flow runs were performed in the absence of CECs. The ozone mass balance at steady-state is given by Equation (8):

$$\beta k_L a (C_{O_3}^* - C_{O_3}) = v_o C_{O_3} + \beta V k_d C_{O_3}, \quad (8)$$

β being the liquid hold-up (0.98), V the total reaction volume, $k_L a$ the volumetric mass-transfer coefficient, $C_{O_3}^*$ and C_{O_3} the ozone concentrations in the interphase and in the liquid bulk, respectively, and v_o the liquid flow rate. Figure 4 shows the aqueous ozone concentration measured in some ozone absorption experiments in continuous mode.

The dissolved ozone concentration reached at the steady-state of the single ozone absorption run ($8.3 \text{ mg}\cdot\text{L}^{-1}$) was taken as the solubility ($C_{O_3}^*$) to be used in Equation (8). From Figure 4 it is apparent that radiation (LED) and, especially, the combination of LED and P25R, enhanced decomposition of the ozone.

According to Charpentier (1981) [31], values of $k_L a$ in packed bubble columns are between 0.005 and 0.12 s^{-1} , giving as a result different k_d values for both photolytic and photocatalytic ozonation as shown in Table 4.

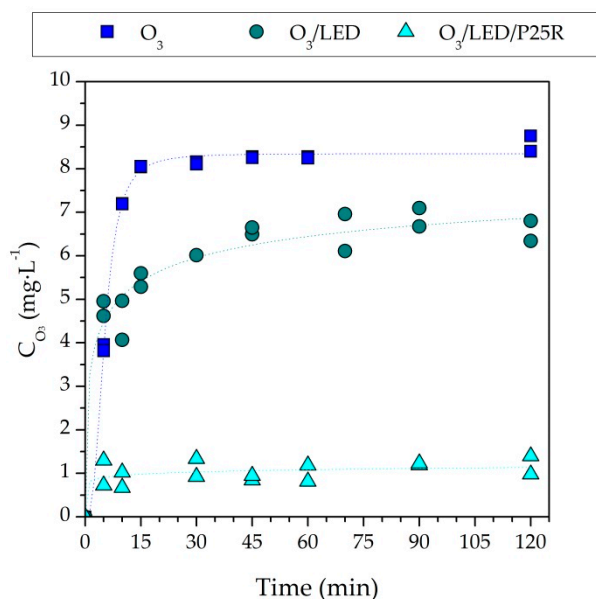


Figure 4. Evolution of dissolved ozone concentration in CEC-free deionized water in continuous operation.

Table 4. Apparent pseudo first order rate constant and Hatta number (Ha) values for ozone decomposition in water in the presence of radiation and radiation/P25R.

k_{La} Values (s^{-1})	O ₃ /LED		O ₃ /LED/P25R	
	k_d (s^{-1})	$Ha_I \times 10^3$	k_d (s^{-1})	$Ha_I \times 10^2$
0.005	1.0×10^{-3}	1.2	3.2×10^{-2}	0.7
0.063	1.7×10^{-2}	5.0	0.40	2.5
0.12	3.3×10^{-2}	7.0	0.77	3.4

$k_d = 8.6 \times 10^{-5} s^{-1}$ and $Ha = 1.8 \times 10^{-4}$ in single ozonation process.

Taking into account the maximum values of k_d constants, the values of Ha_I for the initial ozone decomposition into free radicals at the pH of WW from Equation (7) were all found to be lower than 7.0×10^{-3} (taking the minimum k_{La}) or 3.4×10^{-2} (maximum k_{La}) which, in any case, indicates slow kinetic regimes.

Values of Ha_D for the ozone direct reactions with the contaminants studied here were calculated from Equation (6), and are also presented in Table 2. As can be observed, Ha_D is always lower than 0.1, which indicates a slow kinetic regime for these reactions. Since both ozone reactions (direct and decomposition) develop in the same kinetic regime, there could be potential competition between them for consuming ozone. In order to clarify this point, and following the procedure described in a previous work [33], the ratio between reaction rates of contaminant removal with HO^\bullet and ozone was determined with Equation (9):

$$\frac{r_{HO}}{r_{O_3}} = \frac{k_{HO}k_d}{k_{O_3}\sum C_s k_{HO}} \quad (9)$$

C_s and k_{HO} being the concentration of any other substances present in water that scavenge HO^\bullet and the rate constant of this reaction, respectively. Equation (9) expressed in its logarithmic form [29] is:

$$\log \frac{r_{HO}}{r_{O_3}} = \log \frac{k_{HO}}{k_{O_3}} + \log \frac{k_d}{\sum C_s k_{HO}} \quad (10)$$

Reaction rate ratio (r_{HO}/r_{O_3}) strongly depends on the scavenging factor ($\sum C_s k_{HO}$). This factor was calculated from DOC and inorganic carbon (IC) values in wastewater as reported by Nöthe et al. (2009) [34]. Thus, for WW1 and WW2 values of $\sum C_s k_{HO}$ were found to be $6.7 \times 10^5 s^{-1}$ and $8.2 \times 10^5 s^{-1}$, respectively Figure 5 shows the plot of the reaction rate ratio versus the rate constant

ratio of contaminant-hydroxyl radical and ozone reactions in the ozonation processes. It can be seen from Figure 5 that in all cases the ozone direct reaction rate is much higher than the HO• reaction rate with the contaminant, even for compounds 1, 8, 9, 11, and 12 (bezafibrate, isoproturon, metoprolol, tramadol, and venlafaxine), when treated with O₃/LED/P25R. This confirms that the direct reaction prevails over the hydroxyl radical reaction. However, these compounds (1, 8, 9, 11, and 12) treated with the O₃/LED/P25R system with good mass-transfer coefficient ($k_{L,a} = 0.12 \text{ s}^{-1}$) would be removed mainly by hydroxyl radicals. In summary, the importance of free radical reactions depends on the presence of scavengers in the wastewater to treat. The increase of concentrations of these substances will make the free radical reactions less important compared to the direct ozone reaction and this will depend on the type of AOP. It can be said that the higher the number of hydroxyl radical formation ways, the higher the importance of free radical reactions compared to direct ozone reactions (see Section S1 for initiation reactions of hydroxyl radical formation in AOPs studied).

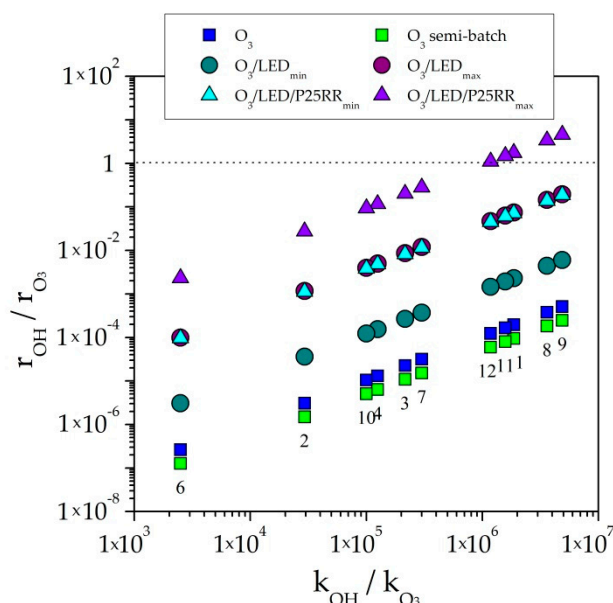


Figure 5. Variation of indirect-direct reaction rate ratio with free radical-direct reaction rate constant ratio with the minimum $k_{L,a}$ (○ and △) in comparison with the maximum $k_{L,a}$ (● and ▲) and semi-batch mode (O₃ □). See Table 1 for meaning of numbers (Plots based on reference [29]).

3. Materials and Methods

Chemicals and solvents (>95% purity) were purchased from different companies and ultrapure water was supplied by a Milli-Q water system. TiO₂ (P25, 80% anatase and 20% rutile crystalline phases) was obtained from Evonik Degussa GmbH. All reference standards (>98% purity) and the isotopically labeled compounds used as internal standards were purchased from Sigma-Aldrich (Steinheim, Germany).

3.1. Wastewater Effluents

Secondary wastewater (WW) samples were collected from a MWWTP located in Northern Portugal and frozen until further use. The main physicochemical parameters are summarized in Table S1, namely pH, dissolved organic carbon (DOC) and inorganic carbon (IC).

3.2. Photocatalysts

Titanium dioxide powder (P25) was used as photocatalyst in semi-batch experiments, and TiO₂-coated glass rings (P25R) were used in continuous flow runs. P25R was prepared as described elsewhere [35]. Briefly, glass rings were immersed in a 5% *w/v* P25-ethanolic solution at a constant

rate of 30 mm/min, in order to create a homogeneous TiO₂ layer. The coated rings were then dried overnight. Since three layers of P25 have been shown to be the optimal number for photocatalytic treatment of water pollutants, the process was repeated two more times and finally P25R were calcined in air at 450 °C for 2 h [35].

3.3. Experimental Set-Up and Procedures

Semi-batch and continuous flow experiments were carried out in this study. Semi-batch mode runs were performed using the experimental set-up schematically shown in Figure 6. As can be seen, the reactor was enclosed in a square box with four 10 W UVA LEDs. Each LED (with maximum irradiance at 390 nm, Figure S2) was provided with a fan for refrigeration purposes. For ozonation runs, ozone was produced from pure oxygen in a BMT 802X ozone generator, and its concentration was monitored with a BMT 964 analyzer. First, the reactor was charged with 750 mL of WW and 0.375 g of P25 (i.e., catalyst concentration of 0.5 g·L⁻¹). The mixture was kept under magnetic agitation in the dark for 10 min to achieve adsorption equilibrium of CECs. Then the LEDs were switched on and a gas stream (150 mL·min⁻¹) of either pure oxygen or an ozone-oxygen mixture (50 mg·L⁻¹ ozone) was bubbled through a ceramic diffuser. After 10 min of reaction, the residual ozone (if ozone was applied) was removed by using an air pump and samples were withdrawn from the reactor to analyze the concentrations of CECs and DOC. In addition to photocatalytic oxidation runs, single ozonation (in the absence of P25 and with LEDs turned off) and photolytic ozonation (in the absence of P25) experiments were carried out for comparative purposes.

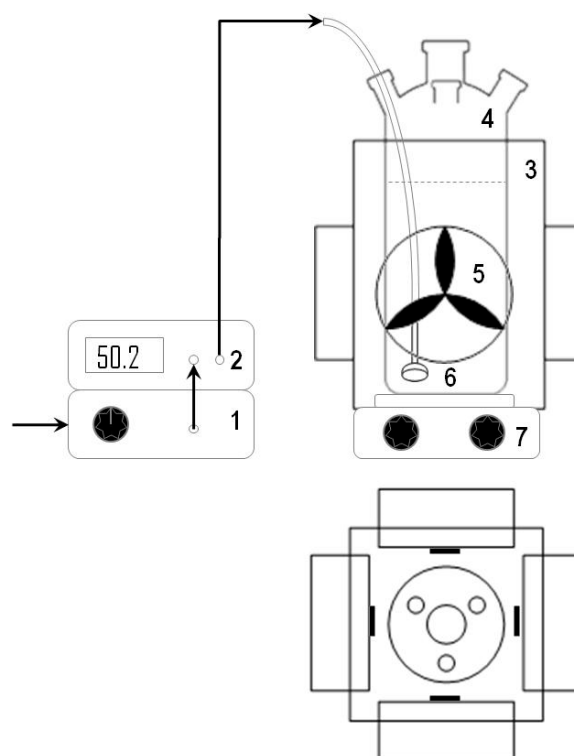


Figure 6. Scheme of the experimental set-up. 1: ozone generator, 2: ozone analyzer, 3: box of LEDs; 4: glass reactor, 5: fan, 6: ceramic diffuser, and 7: magnetic stirrer.

For continuous operation runs the experimental set-up schematically shown in Figure 7 was used. This system consists of a WW reservoir, a glass packed bubble column filled with glass rings (coated with TiO₂ for photocatalytic experiments and uncoated for single and photolytic ozonation runs), a recirculating loop and eight 10 W UVA LEDs positioned along the column (maximum wavelength of emission at 381 nm, Figure S2). Noted that a high concentration of ozone was applied because of the

presence in wastewater of substances different to CECs that are at high concentration (see TOC and IC values in Table S1). These substances also consume ozone and/or hydroxyl radicals. In any case, in a practical situation concentration of ozone could also be in the order of tens of mg L^{-1} [36].

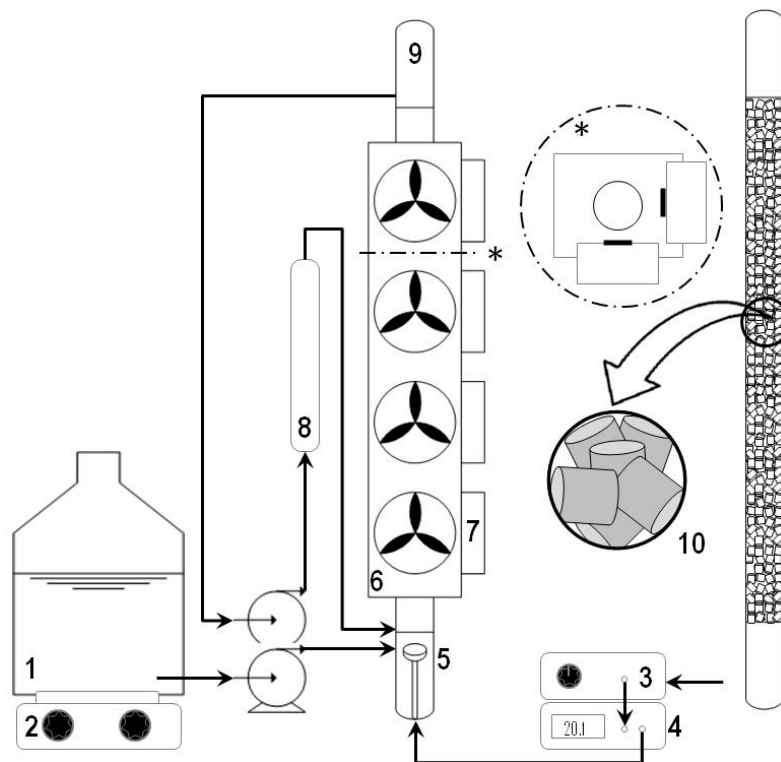


Figure 7. Scheme of the experimental set-up used for continuous operation. 1: reservoir, 2: magnetic stirrer 3: ozone generator, 4: ozone analyzer; 5: ceramic diffuser, 6: box of LEDs, 7: fan, 8: loop column, 9: packed column, and 10: glass coated or uncoated rings. * Cross section of the system. Adapted from [14].

Positive step input tracer experiments were carried out for characterizing the reactor flow pattern. A NaCl aqueous solution ($2 \text{ g}\cdot\text{L}^{-1}$) was used as the tracer. The conductivity of the liquid stream leaving the column was continuously monitored using a Crison GLP 31 conductivity meter to equalize the conductivity value of the inlet solution.

In a typical degradation run, the system was filled with distilled water and then $15 \text{ mL}\cdot\text{min}^{-1}$ of WW were continuously pumped from the reservoir to the column, the recirculation flow rate being set at $166 \text{ mL}\cdot\text{min}^{-1}$. At the same time, a gas flow rate of either oxygen or a mixture of ozone-oxygen ($15 \text{ mL}\cdot\text{min}^{-1}$ and $20 \text{ mg}\cdot\text{L}^{-1}$ ozone) was continuously supplied to the column through a porous diffuser placed at its bottom. LEDs were also turned on (if required). The gas and liquid outlet streams left the system continuously through valves at the top of the reactor. The ozone concentration in the gas stream was continuously monitored while liquid samples were regularly taken from the outlet liquid and immediately bubbled with air to remove residual ozone before analysis. Then the collected samples were centrifuged at 4000 rpm for 5 min prior to the analyses. The removal efficiencies of CECs were evaluated at steady-state.

3.4. Analytical Methods

Concentrations of CECs were measured using an eco-friendly validated method of solid phase extraction followed by ultra-high performance liquid chromatography with tandem mass spectrometry (SPE-UHPLC-MS/MS) described in a previous work [37] where detailed information about recovery percentage of CECs by SPE and precision and accuracy of concentration measurements are given.

Typically, before SPE, 100 mL of WW samples were filtered through 1.2 μm glass microfiber filters GF/C, 47 mm (WhatmanTM), acidified to pH 2 with sulfuric acid and 100 μL of a solution containing internal standards was added. Afterwards, samples were loaded through the conditioned Oasis®HLB cartridges (Hydrophilic-Lipophilic-Balanced sorbent, 150 mg, 6 mL) at a constant flow rate of 10 $\text{mL}\cdot\text{min}^{-1}$, under vacuum. The sample cartridges were then washed with ultrapure water, dried under vacuum and eluted with ethanol. The extracts were evaporated to dryness in a vacuum concentrator and the residues were reconstituted in 400 μL of ethanol and filtered through 0.22 μm polytetrafluoroethylene (PTFE) syringe filters.

Chromatographic analysis was performed using a Shimadzu Corporation UHPLC (Tokio, Japan) equipment provided with two pumps (LC-30AD), an autosampler (SIL-30AC), an oven (CTO-20AC), a degasser (DGU-20A 5R), a system controller (CBM-20A) and the software LC Solution Version 5.41SP1, coupled to a triple quadrupole mass spectrometer detector (Ultra Fast Mass Spectrometry series LCMS-8040). The stationary phase was a KinetexTM 1.7 μm XB-C18 100 Å (100 \times 2.1 mm i.d.) column and a gradient of 0.1% formic acid and methanol at 0.25 $\text{mL}\cdot\text{min}^{-1}$ was programmed as follows: 30:70 (*v/v*) for 0.5 min, a linear gradient from 30:70 (*v/v*) to 10/90 (*v/v*) in 1 min (held for 6 min), a linear gradient from 10:90 (*v/v*) to 30:70 (*v/v*) in 0.5 min and finally an equilibration time of 4 min, with a total run time of 12 min. Column oven and autosampler temperatures were set at 35 °C and 4 °C, respectively. The electrospray ionization source operated in both positive and negative ionization modes. Quantification was performed by selected reaction monitoring (SRM), evaluating the two SRM transitions between the precursor ion and the two most abundant fragment ions for each compound, the most abundant used as quantifier and the second most abundant as qualifier, with a scan time of 100 ms per transition. The capillary voltage, nebulizing and drying gas flows, source and desolvation temperatures were respectively: 4.5 kV, 3.0 $\text{L}\cdot\text{min}^{-1}$, 15 $\text{L}\cdot\text{min}^{-1}$, 250 °C and 400 °C. The collision induced dissociation gas (CID) was Ar at 230 kPa.

DOC was analyzed with a TOC-5000A analyzer (Tokio, Japan), pH was measured with a WTW 703 pH-meter and absorbance at 254 nm was recorded on a TG60 UV-visible spectrophotometer (PG instruments, Lutterworth, England). Dissolved ozone concentration was determined by the indigo method [38].

LEDs irradiance spectra (Figure S2) were obtained using a UV-Vis spectroradiometer (USB2000+ Ocean Optics, Orlando, FL, USA), connected to an optical fiber (QP600-1-SR Ocean Optics) with an irradiance probe on its tip (CC-3-UV-S cosine-corrected irradiance probe, Ocean Optics).

Thickness of P25 layers on P25R samples was determined by scanning electron microscopy (SEM, Quanta 3D FEG (FEI), Billerica, MA, USA) with 20 kV accelerating voltage and a back-scatter electron detector (BSED). Wavelength dispersive X-ray fluorescence (WDXRF, Bruker SB Tiger 4K, Billerica, MA, USA) measurements were carried out in He atmosphere, using XS-5S, PET and LiF(200) crystals and a mask size of 28 mm.

4. Conclusions

CECs found in WW at concentration levels around $\text{ng}\cdot\text{L}^{-1}$, and in some cases $\mu\text{g}\cdot\text{L}^{-1}$, were efficiently removed from municipal secondary wastewater samples by the proposed ozonation-based processes (>90%) except ciprofloxacin, metoprolol, and propranolol in semi-batch experiments. Although few differences were observed between these processes, continuous experiments in deionized water showed that a synergic effect takes place for ozone decomposition with UVA-LED radiation and TiO_2 -coated glass rings, giving rise to a slight enhancement of contaminant removal in the treatment of this municipal wastewater.

In addition, the kinetic study clarified that direct ozone reaction is the main pathway responsible for the removal of CECs. Nevertheless, indirect and direct ozone reaction rates ratios indicate that the HO^\bullet reaction pathway could prevail over direct reaction in the case of the most refractory compounds for the $\text{O}_3/\text{LED}/\text{P25}$ system (i.e., isoproturon).

Consequently, the use of P25 TiO₂-coated rings and energy-efficient LEDs for photocatalytic ozonation could be an attractive way for wastewater treatment in continuous operation.

Additional recommended studies on the AOP treatment of CECs in wastewater are, among others, confirmation of intermediate removals and ozone consumption per TOC removed.

Supplementary Materials: The following are available online at <http://www.mdpi.com/2073-4344/9/5/472/s1>, Table S1: Main characteristics of wastewater samples (WW), Table S2: List of compounds: (i) that can be identified by the SPE-UHPLC-MS/MS method; (ii) listed in 2013/39/EU Directive and/or (iii) 2018/840/EU Decision; and (iv) detected in WW samples, Figure S1: Comparison of removal percentage between WW1 filtered and unfiltered in different semi-batch experiments. Conditions: reaction time = 10 min; gas flow rate = 150 mL·min⁻¹; P25 loading (when applied) = 0.5 g·L⁻¹; ozone concentration = 50 mg·L⁻¹, Figure S2: Irradiance spectra of UVA LEDs used for semi-batch (solid line) and continuous operation (dotted line), Figure S3: Case A: The system behaves as one perfectly mixed reactor. Case B: The system behaves as two perfectly mixed reactors in series due to the reaction column and the recirculation column, Figure S4: F curve versus time from tracer experiment (solid line) and simulated F curves for the reactor set-up in case A (o) and B (Δ), Figure S5: SEM images of fresh coated glass rings surface (A and B). Layer thickness measurements in a polished coated glass ring © and in a scratched coated glass ring surface (D), Table S3: WDXRF results of uncoated glass rings ®, coated glass rings before treatment (P25R) and after photocatalytic oxidation (O₂/LED/P25R) and photocatalytic ozonation (O₃/LED/P25R).

Author Contributions: Conceptualization, A.M.T.S., A.R., P.M.A., and F.J.B.; methodology, A.M.C., A.R.R., and N.F.F.M.; software, A.M.C. and A.R.R.; validation, A.M.C., A.R.R., N.F.F.M., A.M.T.S., A.R., P.M.A., and F.J.B.; formal analysis, A.M.C. and A.R.R.; investigation, A.M.C.; resources, A.M.T.S. and F.J.B.; writing—original draft preparation, A.M.C. and F.J.B.; writing—review and editing, A.M.C.; supervision, A.M.C., A.R.R., N.F.F.M., A.M.T.S., A.R., P.M.A., and F.J.B.; funding acquisition, A.M.T.S. and F.J.B.

Funding: This research was funded by ERDF- European Funds for Regional Development through “MINECO - MINISTERIO DE ECONOMÍA Y COMPETITIVIDAD OF SPAIN, Project CTQ2015-64944-R”, “NORTE 2020 (Programa Operacional Regional do Norte), NORTE-01-0145-FEDER-000006”, “COMPETE2020 - Programa Operacional Competitividade e Internacionalização (POCI) and FCT - Fundação para a Ciência e a Tecnologia, POCI-01-0145-FEDER-006984”.

Acknowledgments: A.M. Chávez, P.M. Álvarez, and F.J. Beltrán are grateful to the MINECO (Project CTQ2015-64944-R), and the ERDF for economically supporting this work. A.M. Chávez gives special thanks to MINECO for her predoctoral grant (call 2013, BES-2013-064186) and mobility grant for a short stay (call 2015, EEBB-I-16-11456). A.M.T. Silva, R. Lado, and N.F.F. Moreira acknowledge Project “AIProcMat@N2020 – Advanced Industrial Processes and Materials for a Sustainable Northern Region of Portugal 2020” (NORTE-01-0145- FEDER-000006), supported by NORTE 2020 (Programa Operacional Regional do Norte), under the Portugal 2020 Partnership Agreement, through the European Funds for Regional Development, and project POCI-01-0145-FEDER-006984 – Associate Laboratory LSRE-LCM funded by ERDF through COMPETE2020 - Programa Operacional Competitividade e Internacionalização (POCI) – and by national funds through FCT - Fundação para a Ciência e a Tecnologia. Besides, N.F.F. Moreira acknowledges financial support from FCT (grant PD/BD/114318/2016).

Conflicts of Interest: The authors declare no conflict of interest.

References

1. Ratola, N.; Cincinelli, A.; Alves, A.; Katsoyiannis, A. Occurrence of organic microcontaminants in the wastewater treatment process. A mini review. *J. Hazard. Mater.* **2012**, *239–240*, 1–18. [[CrossRef](#)]
2. Robles-Molina, J.; Lara-Ortega, F.J.; Gilbert-López, B.; García-Reyes, J.F.; Molina-Díaz, A. Multi-residue method for the determination of over 400 priority and emerging pollutants in water and wastewater by solid-phase extraction and liquid chromatography-time-of-flight mass spectro. *metry. J. Chromatogr. A* **2014**, *1350*, 30–43. [[CrossRef](#)] [[PubMed](#)]
3. Lapworth, D.J.; Baran, N.; Stuart, M.E.; Ward, R.S. Emerging organic contaminants in groundwater: A review of sources, fate and occurrence. *Environ. Pollut.* **2012**, *163*, 287–303. [[CrossRef](#)] [[PubMed](#)]
4. González, S.; López-Roldán, R.; Cortina, J.L. Presence and biological effects of emerging contaminants in Llobregat River basin: A review. *Environ. Pollut.* **2012**, *161*, 83–92. [[CrossRef](#)]
5. Pal, A.; Gin, K.Y.H.; Lin, A.Y.C.; Reinhard, M. Impacts of emerging organic contaminants on freshwater resources: Review of recent occurrences, sources, fate and effects. *Sci. Total Environ.* **2010**, *408*, 6062–6069. [[CrossRef](#)] [[PubMed](#)]

6. Directive 2013/39/EU. Directive 2013/39/EU of the European Parliament and of the Council of 12 August 2013 amending Directives 2000/60/EC and 2008/105/EC as regards priority substances in the field of water policy. *Off. J. Eur. Union.* **2013**, L226, 1–17.
7. Decision 2015/495/EU. Commission implementing decision (EU) 2015/495 of 20 March 2015 establishing a watch list of substances for Union-wide monitoring in the field of water policy pursuant to Directive 2008/105/EC of the European Parliament and of the Council. *Off. J. Eur. Union.* **2015**, L78, 40–42.
8. Decision 2018/840/EU. Commission implementing decision (EU) 2018/840 of 5 June 2018 establishing a watch list of substances for Union-wide monitoring in the field of water policy pursuant to Directive 2008/105/EC of the European Parliament and of the Council. *Off. J. Eur. Union.* **2018**, L141, 9–12.
9. Liu, Z.; Kanjo, Y.; Mizutani, S. Removal mechanisms for endocrine disrupting compounds (EDCs) in wastewater treatment—Physical means, biodegradation, and chemical advanced oxidation: A review. *Sci. Total Environ.* **2008**, *407*, 731–748. [[CrossRef](#)]
10. Gogate, P.R.; Pandit, A.B. A review of imperative technologies for wastewater treatment II: Hybrid methods. *Adv. Environ. Res.* **2004**, *8*, 553–597. [[CrossRef](#)]
11. Von Gunten, U. Ozonation of drinking water: Part I. Oxidation kinetics and product formation. *Water Res.* **2003**, *37*, 1443–1467. [[CrossRef](#)]
12. Legrini, O.; Oliveros, E.; Braun, A.M. Photochemical Processes for Water Treatment. *Chem. Rev.* **1993**, *93*, 671–698. [[CrossRef](#)]
13. Beltrán, F.J. *Ozone Reaction Kinetics for Water and Wastewater Systems*; Lewis Publishers: Boca Raton, FL, USA, 2004; pp. 1–358.
14. Moreira, N.F.F.; Sousa, J.M.; Macedo, G.; Ribeiro, A.R.; Barreiros, L.; Pedrosa, M.; Faria, J.L.; Pereira, M.F.R.; Castro-Silva, S.; Segundo, M.A.; et al. Photocatalytic ozonation of urban wastewater and surface water using immobilized TiO₂ with LEDs: Micropollutants, antibiotic resistance genes and estrogenic activity. *Water Res.* **2016**, *94*, 10–22. [[CrossRef](#)]
15. Lee, Y.; Gerrity, D.; Lee, M.; Encinas Bogeat, A.; Salhi, E.; Gamage, S.; Trenholm, R.A.; Wert, E.C.; Snyder, S.A.; von Gunten, U. Prediction of micropollutant elimination during ozonation of municipal wastewater effluents: Use of kinetic and water specific information. *Environ. Sci. Technol.* **2013**, *47*, 5872–5881. [[CrossRef](#)]
16. Bahr, C.; Schumacher, J.; Ernst, M.; Luck, F.; Heinzmann, B.; Jekel, M. SUVA as control parameter for the effective ozonation of organic pollutants in secondary effluent. *Water Sci. Technol.* **2007**, *55*, 267–274. [[CrossRef](#)]
17. Encinas, A.; Rivas, F.J.; Beltrán, F.J.; Oropesa, A. Combination of black-light photocatalysis and ozonation for emerging contaminants degradation in secondary effluents. *Chem. Eng. Technol.* **2013**, *36*, 492–499. [[CrossRef](#)]
18. Marquez, G.; Rodríguez, E.M.; Beltrán, F.J.; Alvarez, P.M. Solar photocatalytic ozonation of a mixture of pharmaceutical compounds in water. *Chemosphere* **2014**, *113*, 71–78. [[CrossRef](#)]
19. Espejo, A.; Aguinaco, A.; Amat, A.M.; Beltrán, F.J. Some ozone advanced oxidation processes to improve the biological removal of selected pharmaceutical contaminants from urban wastewater. *J. Environ. Sci. Health A* **2014**, *49*, 410–421. [[CrossRef](#)]
20. Gimeno, O.; García-Araya, J.F.; Beltrán, F.J.; Rivas, F.J.; Espejo, A. Removal of emerging contaminants from a primary effluent of municipal wastewater by means of sequential biological degradation-solar photocatalytic oxidation processes. *Chem. Eng. J.* **2016**, *290*, 12–16. [[CrossRef](#)]
21. Dantas, R.F.; Canterino, M.; Marotta, R.; Sans, C.; Esplugas, S.; Andreozzi, R. Bezafibrate removal by means of ozonation: Primary intermediates, kinetics, and toxicity assessment. *Water Res.* **2007**, *41*, 2525–2532. [[CrossRef](#)]
22. Elovitz, M.S.; Von Gunten, U. Hydroxyl radical/ozone ratios during ozonation processes. I. The R(ct) concept. *Ozone Sci. Eng.* **1999**, *21*, 239–260. [[CrossRef](#)]
23. Huber, M.M.; Gbel, A.; Joss, A.; Hermann, N.; Lffler, D.S.C.; Ried, A.; Siegrist, H.; Ternes, T.A.; Gunten, U. Oxidation of pharmaceuticals during ozonation of municipal wastewater effluents: A pilot study. *Environ. Sci. Technol.* **2005**, *39*, 4290–4299. [[CrossRef](#)] [[PubMed](#)]
24. Dodd, M.C.; Buffle, M.O.; Von Gunten, U. Oxidation of antibacterial molecules by aqueous ozone: Moiety-specific reaction kinetics and application to ozone-based wastewater treatment. *Environ. Sci. Technol.* **2006**, *40*, 1969–1977. [[CrossRef](#)]

25. Lee, Y.; Kovalova, L.; McArdell, C.S.; von Gunten, U. Prediction of micropollutant elimination during ozonation of a hospital wastewater effluent. *Water Res.* **2014**, *64*, 134–148. [[CrossRef](#)] [[PubMed](#)]
26. Zhao, Y.; Yu, G.; Chen, S.; Zhang, S.; Wang, B.; Huang, J.; Deng, S.; Wang, Y. Ozonation of antidepressant fluoxetine and its metabolite product norfluoxetine: Kinetics, intermediates and toxicity. *Chem. Eng. J.* **2017**, *316*, 951–963. [[CrossRef](#)]
27. Méndez-Arriaga, F.; Otsu, T.; Oyama, T.; Gimenez, J.; Esplugas, S.; Hidaka, H.; Serpone, N. Photooxidation of the antidepressant drug Fluoxetine (Prozac®) in aqueous media by hybrid catalytic/ozonation processes. *Water Res.* **2011**, *45*, 2782–2794. [[CrossRef](#)]
28. Benitez, F.J.; Real, F.J.; Acero, J.L.; Garcia, C. Kinetics of the transformation of phenyl-urea herbicides during ozonation of natural waters: Rate constants and model predictions. *Water Res.* **2007**, *41*, 4073–4084. [[CrossRef](#)] [[PubMed](#)]
29. Benitez, F.J.; Acero, J.L.; Real, F.J.; Roldán, G. Ozonation of pharmaceutical compounds: Rate constants and elimination in various water matrices. *Chemosphere* **2009**, *77*, 53–59. [[CrossRef](#)]
30. Benner, J.; Salhi, E.; Ternes, T.; von Gunten, U. Ozonation of reverse osmosis concentrate: Kinetics and efficiency of beta blocker oxidation. *Water Res.* **2008**, *42*, 3003–3012. [[CrossRef](#)]
31. Charpentier, J.-C. Mass-transfer rates in gas-liquid absorbers and reactors. In *Advances in Chemical Engineering*; Academic Press: New York, NY, USA, 1981; pp. 1–133.
32. Johnson, P.N.; Davis, R.A. Diffusivity of ozone in water. *J. Chem. Eng. Data.* **1996**, *41*, 1485–1487. [[CrossRef](#)]
33. Beltrán, F.J.; Rey, A. Free radical and direct ozone reaction competition to remove priority and pharmaceutical water contaminants with single and hydrogen peroxide ozonation systems. *Ozone Sci. Eng.* **2018**, *40*, 1–15. [[CrossRef](#)]
34. Nöthe, T.; Fahlenkamp, H.; von Sonntag, C. Ozonation of wastewater: Rate of ozone consumption and hydroxyl radical yield. *Environ. Sci. Technol.* **2009**, *43*, 5990–5995. [[CrossRef](#)]
35. Sampaio, M.J.; Silva, C.G.; Silva, A.M.T.; Vilar, V.J.P.; Boaventura, R.A.R.; Faria, J.L. Photocatalytic activity of TiO₂-coated glass raschig rings on the degradation of phenolic derivatives under simulated solar light irradiation. *Chem. Eng. J.* **2013**, *224*, 32–38. [[CrossRef](#)]
36. Langlais, B.; Reckhow, D.A.; Brink, D.R. (Eds.) *Ozone in Water Treatment: Application and Engineering*; Lewis Publ.: Chelsea, MI, USA, 1991.
37. Ribeiro, A.R.; Pedrosa, M.; Moreira, N.F.F.; Pereira, M.F.R.; Silva, A.M.T. Environmental friendly method for urban wastewater monitoring of micropollutants defined in the Directive 2013/39/EU and Decision 2015/495/EU. *J. Chromatogr. A.* **2015**, *1418*, 140–149. [[CrossRef](#)]
38. Bader, H.; Hoigné, J. Determination of ozone in water by the indigo method. *Water Res.* **1981**, *15*, 449–456. [[CrossRef](#)]

